

Fate of Measurement-Induced Phase Transition in Long-Range Interactions

Takaaki Minato,¹ Koudai Sugimoto¹, Tomotaka Kuwahara,² and Keiji Saito¹¹*Department of Physics, Keio University, Hiyoshi, Kohoku-ku, Yokohama 223-8522, Japan*²*Mathematical Science Team, RIKEN Center for Advanced Intelligence Project (AIP), 1-4-1 Nihonbashi, Chuo-ku, Tokyo 103-0027, Japan*

(Received 14 May 2021; revised 1 November 2021; accepted 2 November 2021; published 5 January 2022)

We consider quantum many-body dynamics under quantum measurements, where the measurement-induced phase transitions (MIPs) occur when changing the frequency of the measurement. In this work, we consider the robustness of the MIP for long-range interaction that decays as $r^{-\alpha}$ with distance r . The effects of long-range interactions are classified into two regimes: (i) the MIP is observed ($\alpha > \alpha_c$), and (ii) the MIP is absent even for arbitrarily strong measurements ($\alpha < \alpha_c$). Using fermion models, we demonstrate both regimes in integrable and nonintegrable cases. We identify the underlying mechanism and propose sufficient conditions to observe the MIP, that is, $\alpha > d/2 + 1$ for general bilinear systems and $\alpha > d + 1$ for general nonintegrable systems (d : spatial dimension). Numerical calculation indicates that these conditions are optimal.

DOI: 10.1103/PhysRevLett.128.010603

Introduction.—Understanding the general properties and finding new phenomena regarding the time evolution of quantum entanglement in quantum many-body systems is a critical subject in physics. Recently, novel dynamic phase transitions in quantum entanglement have been discovered in the presence of quantum measurements [1–22]. In general, the bipartite entanglement entropy of isolated systems grows over time and eventually reaches the order of the system size. Conversely, projective quantum measurements suppress entanglement growth, such as in the quantum Zeno effect under continuous measurement [23]. As a result of this competition, with increasing measurement amplitude (frequency) in nonintegrable systems, the bipartite entanglement entropy in the long-time limit shows a transition from the order of the system size (the volume law phase) to the order of the boundary area (the area law phase). This phenomenon is now referred to as measurement-induced phase transition (MIP).

MIPs have been intensively studied in various systems, such as quantum circuit models [1–15], cold atomic systems [16–19], and quantum spin systems [21,22]. We emphasize that the MIP generally occurs irrespective of integrability or nonintegrability. It has been recently found that free-fermion systems also show the MIP, i.e., a transition between the phase of the entanglement entropy with the order of the logarithmic system size (the sub-volume law phase) and the area law phase [19]. The MIP is believed to be a ubiquitous phenomenon in isolated many-body quantum systems.

In this Letter, we consider the MIP in long-range interacting systems to understand the mechanism more deeply. Here, long-range interaction means that the amplitude of interaction decays as $r^{-\alpha}$, where r is the distance

between particles (see also Ref. [24]). As conceptually established in statistical mechanics [26], phase transitions generally depend on the interaction range, dimensionality, and types of interactions. Various studies have shown that physical properties change qualitatively under long-range interactions. Examples include the static properties of the equilibrium phase [27–29], ground state [30–33], and dynamic properties [34–40]. Thus, it is natural to ask whether long-range interactions influence the physics of MIP.

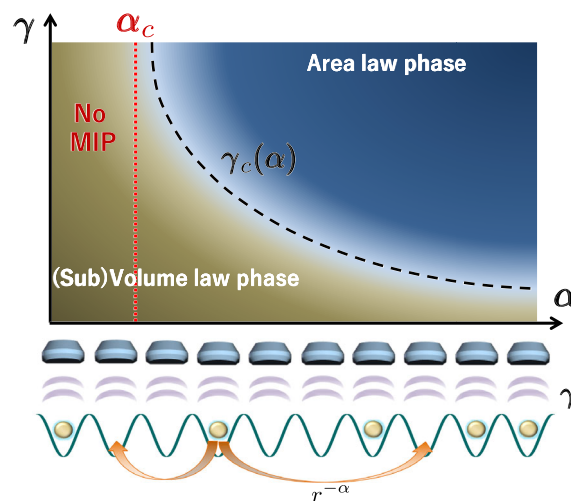


FIG. 1. Schematic of findings. We consider fermion systems with long-range interactions, where each site is constantly measured by the amplitude (frequency) γ . The function $\gamma_c(\alpha)$ is the critical measurement amplitude [see Fig. 3(b) for the free fermion case]. In the regime $\alpha < \alpha_c$, the MIP does not exist. See Statement 1 for sufficient conditions of α for the existence of the MIP.

The long-range interaction immediately propagates the quantum information to particles with arbitrary distances, and hence, the entanglement growth should be enhanced. From this viewpoint, one anticipates nontrivial competition between quantum measurement and long-range interaction strength. We here address the following questions: (i) is there a possibility for the absence of the MIP?; and (ii) what are the conditions for the existence of the MIP?

The primary obstacle to addressing these questions lies in the fact that the dynamics under quantum measurements are highly nonlinear [23], which makes the analyses difficult even numerically. We note that simple Clifford circuit models have been employed in many studies so far to overcome this difficulty [1,2,4–6,12–15]. Following this spirit, we use a simple toy model to grasp the essence. We start with a simple fermion model to address question (i). We then identify the physical mechanism to make a statement applicable to generic systems addressing question (ii), where sufficient conditions to observe the MIP in generic systems are proposed. Then, we obtain several physical pictures, as summarized schematically in Fig. 1.

Model.—To obtain the essential physics of the effect of long-range interaction in the MIP, we consider the following simple long-range Hamiltonian:

$$H = \sum_{j=1}^L \sum_{r=1}^{L/2} \frac{1}{r^\alpha} [-c_{j+r}^\dagger c_j - c_j^\dagger c_{j+r} + V n_{j+r} n_j], \quad (1)$$

where c_j and c_j^\dagger are the annihilation and creation operators of the spinless fermion at site j , and $n_j = c_j^\dagger c_j$, respectively. The parameter α is the degree of long-range interaction. We impose the periodic boundary condition for the total system size L , that is, $c_{j+L} = c_j$. We set the Néel state to the initial state, that is, $\psi(t=0) = \prod_{i=1}^{L/2} c_{2i-1}^\dagger |\text{vac}\rangle$, where $|\text{vac}\rangle$ is the vacuum state. Note that the total number of fermions is fixed at $L/2$ at all times. We perform a quantum measurement uniformly for all sites with a finite measurement amplitude (frequency) γ . Then, the time evolution of the wave function is described by the standard quantum jump process [18,23], that is,

$$d|\psi(t)\rangle = -iH|\psi(t)\rangle dt + \sum_{j=1}^L \left[\frac{c_j^\dagger c_j |\psi(t)\rangle}{\sqrt{\langle \psi(t) | n_j | \psi(t) \rangle}} - |\psi(t)\rangle \right] dw_j(t), \quad (2)$$

where $dw_j(t)$ takes 0 or 1 obeying the site-independent Poisson process, that is, $\langle \langle dw_j(t) \rangle \rangle = \gamma dt$. Here, $\langle \langle \dots \rangle \rangle$ is the noise average. As a result of the measurement process, there are many trajectories of the wave functions starting from the fixed initial state. Hence, we need to take an average over many trajectories to examine the statistical properties of any observables. The main physical quantity

we address is entanglement entropy. Let us divide the system into two subsystems A and B , which have sizes ℓ and $L - \ell$ ($\ell \leq L/2$), respectively. Then, the entanglement entropy is defined as

$$S_\ell := -\text{Tr}(\rho_A \log \rho_A), \quad (3)$$

where ρ_A is the reduced density matrix of subsystem A for a given wave function $|\psi\rangle$, that is, $\rho_A = \text{Tr}_B(|\psi\rangle\langle\psi|)$, where Tr_B is the partial trace with respect to part B . We discuss the trajectory average \bar{S}_ℓ , employing a sufficient number of trajectories. We also compute the mutual information as another indicator to detect the MIP. To this end, we divide the total system into four subsystems in the order of a, b, c , and d along the system [hence, the regions a and d contact with each other on the ring geometry, see also Fig. 2(c)]. We then consider the mutual information between the region a and c , $I(\gamma, \alpha) = S_a + S_c - S_{ac}$, where S_a , S_c , and S_{ac} are the entanglement entropy for the regions a , c , and $a + c$, respectively. We denote the average values of mutual information by $\bar{I}(\gamma, \alpha)$.

Free fermion case.—We first consider the free fermion case, that is, $V = 0$. The wave function can be expressed in the form of $|\psi(t)\rangle = \prod_{m=1}^{L/2} \sum_{j=1}^L u_{j,m}(t) c_j^\dagger |\text{vac}\rangle$. The many-body wave function is expressed through the function $u_{j,m}(t)$, where the relation $\sum_{j=1}^L u_{j,m}^* u_{j,m'} = \delta_{m,m'}$ is imposed to guarantee normalization. The correlation

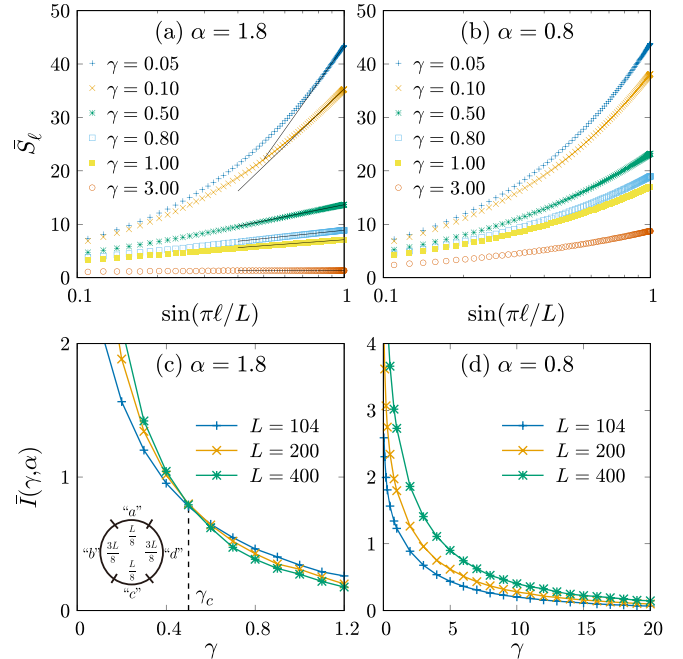


FIG. 2. (a) and (b) \bar{S}_ℓ as a function of $\sin(\pi\ell/L)$ ($L = 200$) for $\alpha = 1.8$ in (a) and for $\alpha = 0.8$ in (b), where the x axis is log scale. The CFT behavior can be observed around $\ell \sim L/2$ as indicated in (a), where the solid lines are guides for the eyes. (c) and (d) The mutual information as a function of γ .

function is calculated using the relation $\langle \psi(t) | c_i^\dagger c_j | \psi(t) \rangle = \sum_{m=1}^{L/2} u_{j,m}(t) u_{i,m}^*(t)$. In addition, the entanglement entropy can be computed once the correlation functions are obtained [41]. See the Supplemental Material for these established methods [42].

In Figs. 2(a) and 2(b), we show the numerical data for the entanglement entropy, which is a long-time average starting from the Néel state. See endnote [43] for the numerical details used to obtain the data. These figures show the ℓ dependence of the entanglement entropy for $\alpha = 1.8$ and $\alpha = 0.8$, respectively, for a fixed length $L = 200$. As indicated in Fig. 2(a) with solid lines, the entanglement entropy around $\ell \sim L/2$ is well fitted by the functional form of the conformal field theory (CFT) with the effective central charge $c(\gamma, \alpha)$: $\bar{S}_\ell = [c(\gamma, \alpha)/3] \log_2[(L/\pi) \sin(\pi\ell/L)] + \text{const.}$. For the short-range interaction limit $\alpha \rightarrow \infty$, this behavior was reported in Ref. [19]. In Fig. 2(a), the entanglement entropies becomes constants for large γ , implying the area law, while Fig. 2(b) has no indication of the area law. Figures 2(c) and 2(d) show the mutual information $\bar{I}(\gamma, \alpha)$ between the regime a and c depicted schematically in Fig. 2(c), where the regions a and c with the length $L/8$ are separated by the regime b and d with the length $3L/8$. Figure 2(c) is the result for $\alpha = 1.8$, where there is a crossing point γ_c , while Fig. 2(d) for $\alpha = 0.8$ does not exhibit such a crossing phenomenon.

For the free fermion model, the finite-size effect is significant [19], and hence it is not trivial to obtain critical points which separate the subvolume law phase (nonzero central charge in \bar{S}_ℓ) and the area law phase (constants in $\bar{S}_{L/2}$). To suppress the size effects, we use crossing points as illustrated in Fig. 2(c) to detect the critical points. In addition, we consider the Berezinskii-Kosterlitz-Thouless (BKT) scenario that was valid for the short-range limit [19]. We remark that a similar technique using crossing points has been employed for several equilibrium systems [44,45]. Note also that the mutual information has been employed as a good indicator to detect the MIP in many systems [4,10,18]. We use an ansatz of the finite-size scaling for the BKT scenario [19,46,47]: $g(L)\gamma\bar{I}(\gamma, \alpha) = F(\log\{L\xi[\gamma, \gamma_c(\alpha)]\})$, where ξ is the BKT-type correlation length $\xi[\gamma, \gamma_c(\alpha)] \sim \exp[-\nu/\sqrt{\gamma - \gamma_c(\alpha)}]$. Here, $\gamma_c(\alpha)$ is the crossing point, which depends on α . In Fig. 3(a), we verified that the scaling ansatz. These scaling data strongly suggest that γ_c can be regarded as critical points. In Fig. 3(b), we show the behavior of $\gamma_c(\alpha)$ as a function of α . In the gray shaded area ($\alpha < 1.5$), we can find no critical points [that is, no crossing point, as shown in Fig. 2(d) [42]]. Thus, we find that the critical value $\alpha_c \simeq 1.5$ separates the absence and existence of the MIP (see Fig. 1).

Analysis based on the entanglement growth rate.—Next, we discuss the underlying physical mechanism for the numerical findings in Fig. 3(b). We argue that the key component is the growth rate of the entanglement entropy

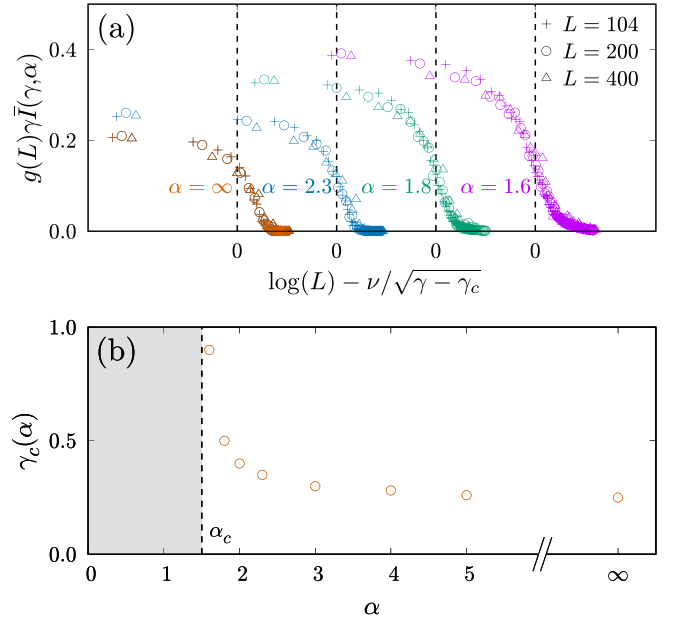


FIG. 3. (a) Finite-size scaling for the mutual information with the BKT scenario $g(L)\gamma\bar{I}(\gamma, \alpha)$ versus $\log\{L\xi[\gamma, \gamma_c(\alpha)]\} = \log L - \nu/\sqrt{\gamma - \gamma_c(\alpha)}$, where $\nu = 6.0, 5.5, 4.5$, and 3.0 for $\alpha = 1.6, 1.8, 2.3$, and $\alpha = \infty$, respectively and $g(L) = [1 + 1/(2 \log L - 4)]^{-1}$. (b) Critical amplitude $\gamma_c(\alpha)$ as a function of α . No critical amplitude exists for $\alpha < 1.5$.

in pure quantum dynamics without measurement. Note the following expression for the entropy growth rate under pure quantum dynamics:

$$\begin{aligned} \dot{S}_\ell &= -i \|H_{AB}\| \lambda(\rho), \\ \lambda(\rho) &:= \text{Tr}(h_{AB}[\rho, \log \rho_A \otimes \mathbf{1}_B]), \end{aligned} \quad (4)$$

where $\rho = |\psi(t)\rangle\langle\psi(t)|$, $h_{AB} := H_{AB}/\|H_{AB}\|$ ($\|\dots\|$ is the operator norm), and $\mathbf{1}_B$ is the identity operator for subsystem B . The Hamiltonian H_{AB} denotes the boundary interaction between subsystems A and B :

$$H_{AB} = \sum_{i \in A} \sum_{j \in B} h_{i,j}, \quad (5)$$

where $h_{i,j}$ is an interaction operator acting on sites i and j . Of interest is the case where $\ell = L/2$. While the function $\lambda(\rho)$ highly depends on the states [48–50], the value is finite for less entangled states (it is zero, especially for a decoupled state such as the Néel state). Suppose that $\|H_{AB}\|$ is finite. Then, a sufficiently large measurement amplitude can suppress the entanglement growth, and hence the MIP should occur. Conversely, when $\|H_{AB}\|$ diverges in the thermodynamic limit, the finite measurement amplitude can no longer suppress entanglement growth, leading to the absence of the MIP. Therefore, the operator norm $\|H_{AB}\|$ should play a central role in determining the presence or absence of MIPs. We

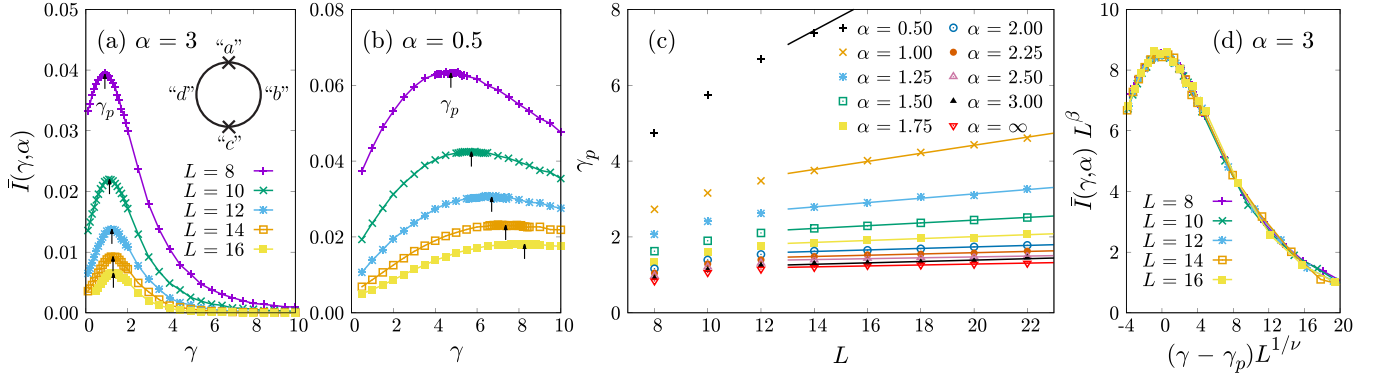


FIG. 4. (a) and (b) The mutual information $\bar{I}(\gamma, \alpha)$ between the farthest two sites for $\alpha = 3.0$ in (a) and for $\alpha = 0.5$ in (b). The values γ_p indicated by arrows are amplitudes that give the peaks. (c) The system-size dependence of γ_p . This indicates that γ_p robustly remains finite for $\alpha > 2$ in the thermodynamic limit. (d) The finite-size scaling for $\alpha = 3.0$ with the ansatz $\bar{I}(\gamma, \alpha) = L^{-\beta} f[(\gamma - \gamma_p)L^{1/\nu}]$ with the exponents $\beta = 2.59 \pm 0.02$ and $\nu = 1.4 \pm 0.1$.

consider the size dependence of the operator norm $\|H_{AB}\|$ for $\ell = L/2$ in the free fermion case. We numerically find that $\|H_{AB}\| \propto L^{1-\alpha}$ ($\alpha < 1$), $\propto \log L$ ($1 < \alpha < 1.5$) and constants ($\alpha > 1.5$) (see also Fig. S3 in the Supplemental Material [42]). This explains the absence of MIP for $\alpha < 1.5$ in Fig. 3(b).

Sufficient condition for the MIP in generic systems.—The free fermion model indicates that the behavior of the boundary interaction Hamiltonian is a key component for observing the MIP, as it governs the entanglement growth rate under pure quantum dynamics, and we now use this key component to make a statement applicable to generic systems. We discuss the sufficient conditions to observe the MIP for generic fermion systems. That is, we seek the value $\alpha_{sc} (\geq \alpha_c)$, where for $\alpha > \alpha_{sc}$, the MIP exists for generic many-body quantum systems. To this end, we rigorously derive the following lemma:

Lemma 1.—Let us consider a Hamiltonian on the d -dimensional hypercubic lattice as $H = \sum_{i<j} h_{i,j}$ such that $\|h_{i,j}\| \leq g/r_{i,j}^\alpha$, where g is a constant. Then, under the condition of $\alpha > \alpha_{sc}$ with

$$\alpha_{sc} = \begin{cases} d/2 + 1 & \text{Bilinear systems,} \\ d + 1 & \text{Interacting systems,} \end{cases} \quad (6)$$

the operator norm $\|H_{AB}\|$ is upper bounded by the boundary area between A and B .

See the Supplemental Material for rigorous proof [42]. Using this lemma and the underlying physics, we can make a physical statement regarding the existence of the MIP:

Statement 1.— $\alpha > \alpha_{sc}$ is a sufficient condition for the existence of the MIP for generic uniform and noncommuting systems.

Note that the statement is the sufficient condition for any system to have the MIP, and hence, this does not exclude that specific models can show the MIP for $\alpha < \alpha_{sc}$.

True critical value for a specific model, α_c , is equal to or smaller than the value α_{sc} . Intriguingly, in the bilinear fermion system that we have discussed, the above statement is optimal, since $\alpha_c = \alpha_{sc} = 3/2$.

Interacting fermion systems.—In the remainder of this Letter, we demonstrate that the above statement is satisfied in nonintegrable models. We consider the interacting fermion system with $V = 1$ in Eq. (1). We first calculate the operator norm $\|H_{AB}\|$ up to the size $L = 256$ using the density-matrix renormalization group technique [51–53]. We find clear evidence that $\|H_{AB}\| \propto L^{2-\alpha}$ for $\alpha < 2$, while they are constants for $\alpha > 2$ (see Fig. S4 in the Supplemental Material [42]), from which we anticipate that the MIP appears for $\alpha > 2$, which is consistent with Statement 1.

To assess this statement in greater detail, we perform the time-evolution calculation up to the system size $L = 22$ using the time-dependent variational principle method [54–56]. See the footnote for the numerical details [57]. We focus on the mutual information $\bar{I}(\gamma, \alpha)$ between the farthest two sites a and c that is depicted in Fig. 4(a), where the regimes b and d have $L/2 - 1$ sites.

We show the results for $\alpha = 3.0$ and $\alpha = 0.5$ in Figs. 4(a) and 4(b), respectively, as functions of γ for different system sizes. To discuss the figures, we recall that many studies so far [4,10,18] have established that in nonintegrable systems, the mutual information shows a peak as a function of γ , where the amplitude giving a peak denoted by γ_p is identified as a critical value of the measurement amplitude separating the volume law phase for $\gamma < \gamma_p$, and the area law phase for $\gamma > \gamma_p$ in the thermodynamic limit. Figures 4(a) and 4(b) also show the peak structure as a function of γ . However, a crucial observation here is that the values of γ_p (indicated by arrows) generally depend on the system size. In the case of $\alpha = 3.0$, the values of γ_p are not affected by the system size, especially for large L .

For $\alpha = 0.5$, the values of γ_p are strongly affected by the system size, that is, γ_p systematically increases with increasing system size.

This systematic change for $\alpha = 0.5$ indicates that γ_p eventually diverges in the thermodynamic limit, leading to the absence of the MIP. From this observation, the system-size dependence of γ_p should be an indicator of the existence of the MIP. In Fig. 4(c), we plot the values of γ_p as a function of the system size L for various α values. This figure shows that for $\alpha > 2$, γ_p is robustly finite for sufficiently large system sizes, which means that the critical measurement amplitude exists even in the thermodynamic limit; hence, the MIP shows up for (at least) $\alpha > 2$. This observation is consistent with Statement 1, which states that $\alpha > 2$ is sufficient to observe the MIP in one-dimensional generic interacting systems. As an additional check on the existence of the MIP for $\alpha > 2$, we consider the finite-size scaling with the ansatz $\bar{I}(\gamma, \alpha) = L^{-\beta} f[(\gamma - \gamma_p)L^{1/\nu}]$. In Fig. 4(d), we show that the finite-size scaling works well with the exponents $\beta = 2.59 \pm 0.02$ and $\nu = 1.4 \pm 0.1$. Note that for $\alpha < 2$, this scaling is not available since γ_p varies as increasing the size. Available analysis for given data are consistent with Statement 1. In the present interacting system, the sufficient condition is optimal, since $\alpha_{sc} = \alpha_c = 2$.

Summary.—We have revealed the effects of long-range interactions on the measurement-induced phase transition (MIP), which is summarized in Fig. 1. The key component for the existence of the MIP is the boundary interaction Hamiltonian under pure quantum dynamics in the thermodynamic limit. Based on this, we have arrived at sufficient conditions to observe the MIP, as described in Statement 1. The numerical results for the specific models indicate that this condition is optimal. We hope that this criterion is useful in real experimental setup with long-range interaction [58–70].

We are grateful to Yohei Fuji, Michael Buchhold, and Sebastian Diehl for providing details regarding their papers and useful suggestions. We also thank Seiji Miyashita for his useful comments on the BKT scaling. K. Sugimoto was supported by Japan Society for the promotion of science (JP19K14644, JP20H01849). T.K. was supported by the RIKEN Center for AIP and JSPS KAKENHI (Grant No. JP18K13475). K. Saito was supported by Japan Society for the promotion of science (JP19H05603, JP19H05791).

Note added.—Recently, we became aware of complementary works on the measurement-induced phase transition using long-range quantum circuits [71] and on the field theoretical argument for the free fermion systems [72]. The latter work [72] is related to our sufficient condition in Statement 1 and some classification of phase transitions is shown.

- [1] Y. Li, X. Chen, and M. P. A. Fisher, Quantum Zeno effect and the many-body entanglement transition, *Phys. Rev. B* **98**, 205136 (2018).
- [2] A. Chan, R. M. Nandkishore, M. Pretko, and G. Smith, Unitary-projective entanglement dynamics, *Phys. Rev. B* **99**, 224307 (2019).
- [3] B. Skinner, J. Ruhman, and A. Nahum, Measurement-Induced Phase Transitions in the Dynamics of Entanglement, *Phys. Rev. X* **9**, 031009 (2019).
- [4] Y. Li, X. Chen, and M. P. A. Fisher, Measurement-driven entanglement transition in hybrid quantum circuits, *Phys. Rev. B* **100**, 134306 (2019).
- [5] M. J. Gullans and D. A. Huse, Dynamical Purification Phase Transition Induced by Quantum Measurements, *Phys. Rev. X* **10**, 041020 (2020).
- [6] M. J. Gullans and D. A. Huse, Scalable Probes of Measurement-Induced Criticality, *Phys. Rev. Lett.* **125**, 070606 (2020).
- [7] C.-M. Jian, Y.-Z. You, R. Vasseur, and A. W. W. Ludwig, Measurement-induced criticality in random quantum circuits, *Phys. Rev. B* **101**, 104302 (2020).
- [8] Y. Bao, S. Choi, and E. Altman, Theory of the phase transition in random unitary circuits with measurements, *Phys. Rev. B* **101**, 104301 (2020).
- [9] S. Choi, Y. Bao, X.-L. Qi, and E. Altman, Quantum Error Correction in Scrambling Dynamics and Measurement-Induced Phase Transition, *Phys. Rev. Lett.* **125**, 030505 (2020).
- [10] M. Sznyszewski, A. Romito, and H. Schomerus, Entanglement transition from variable-strength weak measurements, *Phys. Rev. B* **100**, 064204 (2019).
- [11] R. Fan, S. Vijay, A. Vishwanath, and Y.-Z. You, Self-organized error correction in random unitary circuits with measurement, *Phys. Rev. B* **103**, 174309 (2021).
- [12] S. Vijay, Measurement-driven phase transition within a volume-law entangled phase, [arXiv:2005.03052](https://arxiv.org/abs/2005.03052).
- [13] A. Lavasani, Y. Alavirad, and M. Barkeshli, Measurement-induced topological entanglement transitions in symmetric random quantum circuits, *Nat. Phys.* **17**, 342 (2021).
- [14] S. Sang and T. H. Hsieh, Measurement-protected quantum phases, *Phys. Rev. Research* **3**, 023200 (2021).
- [15] M. Ippoliti, M. J. Gullans, S. Gopalakrishnan, D. A. Huse, and V. Khemani, Entanglement Phase Transitions in Measurement-Only Dynamics, *Phys. Rev. X* **11**, 011030 (2021).
- [16] Q. Tang and W. Zhu, Measurement-induced phase transition: A case study in the nonintegrable model by density-matrix renormalization group calculations, *Phys. Rev. Research* **2**, 013022 (2020).
- [17] S. Goto and I. Danshita, Measurement-induced transitions of the entanglement scaling law in ultracold gases with controllable dissipation, *Phys. Rev. A* **102**, 033316 (2020).
- [18] Y. Fuji and Y. Ashida, Measurement-induced quantum criticality under continuous monitoring, *Phys. Rev. B* **102**, 054302 (2020).
- [19] O. Alberton, M. Buchhold, and S. Diehl, Entanglement Transition in a Monitored Free-Fermion Chain: From Extended Criticality to Area Law, *Phys. Rev. Lett.* **126**, 170602 (2021).

- [20] L. Fidkowski, J. Haah, and M. B. Hastings, How dynamical quantum memories forget, *Quantum* **5**, 382 (2021).
- [21] X. Turkeshi, R. Fazio, and M. Dalmonte, Measurement-induced criticality in $(2 + 1)$ -dimensional hybrid quantum circuits, *Phys. Rev. B* **102**, 014315 (2020).
- [22] N. Lang and H. P. Büchler, Entanglement transition in the projective transverse field Ising model, *Phys. Rev. B* **102**, 094204 (2020).
- [23] H. M. Wiseman and G. J. Milburn, *Quantum Measurement and Control* (Cambridge University Press, Cambridge, England, 2009).
- [24] As in Ref. [25], a quantum circuit model with randomly selected networks can also be called a long-range interacting model. However, it is not relevant to ours because the system we address here is a Hamiltonian system, where each particle simultaneously interacts with the rest of the particles depending on the distance.
- [25] A. Nahum, S. Roy, B. Skinner, and J. Ruhman, Measurement and entanglement phase transitions in all-to-all quantum circuits, on quantum trees, and in Landau-Ginsburg theory, *Phys. Rev. X Quantum* **2**, 010352 (2021).
- [26] E. M. Lifshitz and L. P. Pitaevskii, *Statistical Physics: Theory of the Condensed State* (Elsevier, New York, 2013), Vol. 9.
- [27] F. J. Dyson, Existence of a phase-transition in a one-dimensional Ising ferromagnet, *Commun. Math. Phys.* **12**, 91 (1969).
- [28] D. J. Thouless, Long-range order in one-dimensional Ising systems, *Phys. Rev.* **187**, 732 (1969).
- [29] J. M. Kosterlitz, Phase Transitions in Long-Range Ferromagnetic Chains, *Phys. Rev. Lett.* **37**, 1577 (1976).
- [30] T. Kuwahara and K. Saito, Area law of noncritical ground states in 1d long-range interacting systems, *Nat. Commun.* **11**, 4478 (2020).
- [31] T. Koffel, M. Lewenstein, and L. Tagliacozzo, Entanglement Entropy for the Long-Range Ising Chain in a Transverse Field, *Phys. Rev. Lett.* **109**, 267203 (2012).
- [32] D. Vodola, L. Lepori, E. Ercolessi, A. V. Gorshkov, and G. Pupillo, Kitaev Chains with Long-Range Pairing, *Phys. Rev. Lett.* **113**, 156402 (2014).
- [33] D. Vodola, L. Lepori, E. Ercolessi, and G. Pupillo, Long-range Ising and Kitaev models: Phases, correlations and edge modes, *New J. Phys.* **18**, 015001 (2015).
- [34] C.-F. Chen and A. Lucas, Finite Speed of Quantum Scrambling with Long Range Interactions, *Phys. Rev. Lett.* **123**, 250605 (2019).
- [35] M. C. Tran, C.-F. Chen, A. Ehrenberg, A. Y. Guo, A. Deshpande, Y. Hong, Z.-X. Gong, A. V. Gorshkov, and A. Lucas, Hierarchy of Linear Light Cones with Long-Range Interactions, *Phys. Rev. X* **10**, 031009 (2020).
- [36] T. Kuwahara and K. Saito, Strictly Linear Light Cones in Long-Range Interacting Systems of Arbitrary Dimensions, *Phys. Rev. X* **10**, 031010 (2020).
- [37] T. Zhou, S. Xu, X. Chen, A. Guo, and B. Swingle, Operator Lévy Flight: Light Cones in Chaotic Long-Range Interacting Systems, *Phys. Rev. Lett.* **124**, 180601 (2020).
- [38] S. Tamaki and K. Saito, Energy current correlation in solvable long-range interacting systems, *Phys. Rev. E* **101**, 042118 (2020).
- [39] T. Kuwahara and K. Saito, Absence of Fast Scrambling in Thermodynamically Stable Long-Range Interacting Systems, *Phys. Rev. Lett.* **126**, 030604 (2021).
- [40] R. M. Nandkishore and S. Lal Sondhi, Many-Body Localization with Long-Range Interactions, *Phys. Rev. X* **7**, 041021 (2017).
- [41] J. Eisert, M. Cramer, and M. B. Plenio, Colloquium: Area laws for the entanglement entropy, *Rev. Mod. Phys.* **82**, 277 (2010).
- [42] See Supplemental Material at <http://link.aps.org/supplemental/10.1103/PhysRevLett.128.010603> for the details of the numerical calculation and derivation of the Lemma 1.
- [43] Numerical details: We set the relaxation time to $t = 30$. We use 10^5 trajectories for averaging. For each trajectory, we shift the coordinate of sites along the ring to take more average. Totally, we use $L \times 10^5$ samples to obtain \bar{S} .
- [44] J. Carrasquilla and M. Rigol, Superfluid to normal phase transition in strongly correlated bosons in two and three dimensions, *Phys. Rev. A* **86**, 043629 (2012).
- [45] M. Nishino and S. Miyashita, Termination of the Berezinskii-Kosterlitz-Thouless phase with a new critical universality in spin-crossover systems, *Phys. Rev. B* **92**, 184404 (2015).
- [46] A. W. Sandvik, Computational studies of quantum spin systems, in *AIP Conference Proceedings* (American Institute of Physics, 2010), Vol. 1297, pp. 135–338.
- [47] K. Harada and N. Kawashima, Universal jump in the helicity modulus of the two-dimensional quantum XY model, *Phys. Rev. B* **55**, R11949 (1997).
- [48] K. Van Acoleyen, M. Mariën, and F. Verstraete, Entanglement Rates and Area Laws, *Phys. Rev. Lett.* **111**, 170501 (2013).
- [49] C. H. Bennett, A. Wettroth Harrow, D. W. Leung, and J. A. Smolin, On the capacities of bipartite hamiltonians and unitary gates, *IEEE Trans. Inf. Theory* **49**, 1895 (2003).
- [50] S. Bravyi, Upper bounds on entangling rates of bipartite hamiltonians, *Phys. Rev. A* **76**, 052319 (2007).
- [51] S. R. White, Density Matrix Formulation for Quantum Renormalization Groups, *Phys. Rev. Lett.* **69**, 2863 (1992).
- [52] S. R. White, Density-matrix algorithms for quantum renormalization groups, *Phys. Rev. B* **48**, 10345 (1993).
- [53] U. Schollwöck, The density-matrix renormalization group in the age of matrix product states, *Ann. Phys. (Amsterdam)* **326**, 96 (2011).
- [54] J. Haegeman, J. I. Cirac, T. J. Osborne, I. Pižorn, H. Verschelde, and F. Verstraete, Time-Dependent Variational Principle for Quantum Lattices, *Phys. Rev. Lett.* **107**, 070601 (2011).
- [55] J. Haegeman, T. J. Osborne, and F. Verstraete, Post-matrix product state methods: To tangent space and beyond, *Phys. Rev. B* **88**, 075133 (2013).
- [56] M. Yang and S. R. White, Time-dependent variational principle with ancillary Krylov subspace, *Phys. Rev. B* **102**, 094315 (2020).
- [57] The truncation error is set to be smaller than 10^{-10} , and after each measurement, we enlarge the bond dimension of the matrix-product state using the global-subspace expansion method [56]. For each system size, we use the same number of trajectories as in the free fermion case [43].

- [58] V. Bendkowsky, B. Butscher, J. Nipper, J. P. Shaffer, R. Löw, and T. Pfau, Observation of ultralong-range rydberg molecules, *Nature (London)* **458**, 1005 (2009).
- [59] I. Bloch, J. Dalibard, and W. Zwerger, Many-body physics with ultracold gases, *Rev. Mod. Phys.* **80**, 885 (2008).
- [60] M. Saffman, T. G. Walker, and K. Mølmer, Quantum information with rydberg atoms, *Rev. Mod. Phys.* **82**, 2313 (2010).
- [61] B. Yan, S. A. Moses, B. Gadway, J. P. Covey, K. R. A. Hazzard, A. M. Rey, D. S. Jin, and J. Ye, Observation of dipolar spin-exchange interactions with lattice-confined polar molecules, *Nature (London)* **501**, 521 (2013).
- [62] K. Aikawa, A. Frisch, M. Mark, S. Baier, A. Rietzler, R. Grimm, and F. Ferlaino, Bose-Einstein Condensation of Erbium, *Phys. Rev. Lett.* **108**, 210401 (2012).
- [63] J. W. Britton, B. C. Sawyer, A. C. Keith, C.-C. J. Wang, J. K. Freericks, H. Uys, M. J. Biercuk, and J. J. Bollinger, Engineered two-dimensional Ising interactions in a trapped-ion quantum simulator with hundreds of spins, *Nature (London)* **484**, 489 (2012).
- [64] R. Islam, C. Senko, W. C. Campbell, S. Korenblit, J. Smith, A. Lee, E. E. Edwards, C.-C. J. Wang, J. K. Freericks, and C. Monroe, Emergence and frustration of magnetism with variable-range interactions in a quantum simulator, *Science* **340**, 583 (2013).
- [65] J. Zeiher, R. Van Bijnen, P. Schauß, S. Hild, J.-Y. Choi, T. Pohl, I. Bloch, and C. Gross, Many-body interferometry of a rydberg-dressed spin lattice, *Nat. Phys.* **12**, 1095 (2016).
- [66] J. Zeiher, J.-Y. Choi, A. Rubio-Abadal, T. Pohl, R. Van Bijnen, I. Bloch, and C. Gross, Coherent Many-Body Spin Dynamics in a Long-Range Interacting Ising Chain, *Phys. Rev. X* **7**, 041063 (2017).
- [67] H. Bernien, S. Schwartz, A. Keesling, H. Levine, A. Omran, H. Pichler, S. Choi, A. S. Zibrov, M. Endres, M. Greiner *et al.*, Probing many-body dynamics on a 51-atom quantum simulator, *Nature (London)* **551**, 579 (2017).
- [68] J. Zhang, G. Pagano, P. W. Hess, A. Kyprianidis, P. Becker, H. Kaplan, A. V. Gorshkov, Z.-X. Gong, and C. Monroe, Observation of a many-body dynamical phase transition with a 53-qubit quantum simulator, *Nature (London)* **551**, 601 (2017).
- [69] B. Neyenhuis, J. Zhang, P. W. Hess, J. Smith, A. C. Lee, P. Richerme, Z.-X. Gong, A. V. Gorshkov, and C. Monroe, Observation of prethermalization in long-range interacting spin chains, *Sci. Adv.* **3**, e1700672 (2017).
- [70] F. Liu, R. Lundgren, P. Titum, G. Pagano, J. Zhang, C. Monroe, and A. V. Gorshkov, Confined Quasiparticle Dynamics in Long-Range Interacting Quantum Spin Chains, *Phys. Rev. Lett.* **122**, 150601 (2019).
- [71] M. Block, Y. Bao, S. Choi, E. Altman, and N. Y. Yao, following Letter, Measurement-Induced Transition in Long-Range Interacting Quantum Circuits, *Phys. Rev. Lett.* **128**, 010604 (2022).
- [72] T. Müller, S. Diehl, and M. Buchhold, this issue, Measurement-Induced Dark State Phase Transitions in Long-Ranged Fermion Systems, *Phys. Rev. Lett.* **128**, 010605 (2022).